Electronic band structures for zinc-blende and wurtzite CdS

K. J. Chang, Sverre Froyen, and Marvin L. Cohen
Department of Physics, University of California, Berkeley, California 94720
and Materials and Molecular Research Division, Lawrence Berkeley Laboratory, Berkeley, California 94720
(Received 23 May 1983)

The electronic band structures for zinc-blende and wurtzite CdS are calculated within the local-density approximation with the use of first-principles pseudopotentials. Incorporating the *d* state into the valence band improves substantially the main-valence-band width, and yields valence-band features in good agreement with experiment. The maximum effect of the *d* band occurs at Γ_{15} for zinc-blende CdS and at Γ_1, Γ_6 for wurtzite CdS. We find that the local-density approximation does not predict accurately the position of localized Cd 4*d* state.

I. INTRODUCTION

Recent experimental work[1] on hexagonal CdS using angle-resolved photoemission spectroscopy (ARPES) has provided important information in elucidating the valence-band structure of this material and wurtzite compounds in general. As a result of ARPES, previous theoretical calculations[2,3] have been shown to give an inadequate description of the valence-band features of hexagonal CdS.

The cubic[4] and hexagonal[5] phases of CdS have been studied experimentally. Investigations of the electronic structural properties of CdS, and the ultraviolet (uv) reflectivity spectra observed in bulk hexagonal[6] and in epitaxially grown cubic[7] CdS, have shown that the fundamental band gaps in both structures differ by less than 0.1 eV. X-ray photoemission spectroscopy[8] (XPS) has been performed to study the valence-band features of hexagonal CdS, and an upper valence-band width of 5.0 eV has been reported. Recently Stoffel and Margaritondo[1] have measured valence-band energies of CdS in the wurtzite structure at the high-symmetry points using ARPES. This experiment assigns a main valence-band width of 4.5 eV, in good agreement with the XPS data. The position of the CdS *d* band has been reported to be located within the valence bands of this material about 9.64—10.7 eV below the top of the valence band.[8–11]

On the theoretical side, there have been many reports[12–15] on cubic CdS whereas only two band-structure calculations[2,3] were done for the wurtzite structure over 15 years ago. The difficulty in the theoretical determination of the wurtzite band structure compared to the cubic modification results from the fact that this structure has twice the number of atoms per unit cell and lower symmetry because of the hexagonal anisotropy. For cubic CdS the calculations[12–14] using the orthogonalized-plane-wave (OPW) method, in which the *d* band is included as a valence state, have seriously underestimated the upper-valence-band width. With the use of linear combination of atomic orbitals (LCAO) method[15] including the *d* band, Zunger and Freeman reported the main-valence-band width of 5.1 eV for cubic CdS, but the band gap was underestimated by 0.5 eV. For CdS in the wurtzite structure, the OPW (Ref. 2) and the empirical pseudopotential method[3] (EPM) have predicted the band gap and the optical transition spectra in good agreement with the experiments. However, both calculations seriously underestimated the main-valence-band width (3.3 eV in the OPW and 3.0 eV in the EPM), and there are additional differences between these caluclations and the ARPES results in the upper-valence-band region at high-symmetry points. Further, the *d* band has not been predicted accurately. The EPM did not include the *d* electrons and the OPW calculation placed the *d* band 7 eV below the recently measured values. This error is probably caused by poor calculational convergence.

Most recent electronic band-structure calculations have employed the local-density approximation (LDA).[16] The LDA has been shown to be a good approximation for calculating the ground-state properties. However, this approach fails to describe accurately localized core and excited states.[17] Nevertheless, since this first-principles theory usually provides good qualitative descriptions of these states, we have used the LDA in the present calculation. The purpose of this work is to calculate the self-consistent electronic band structures for CdS in both the cubic and hexagonal structures, and to make detailed comparisons with previous calculations and with experiments.

In Sec. II we briefly describe the method generating the relativistic pseudopotentials and the results of the tests for accuracy. In Sec. III the atomic structures of Cd and S are compared for several different formulations of the exchange-correlation functional. The calculated results for the band structures, including the relativistic and the *d*-band effects, are presented and compared with experimental and other theoretical results. A discussion of the effects of the *d-p* and *d-s* interactions on the band structure is also given. Finally, Sec. IV contains a summary of this work.

II. PSEUDOPOTENTIAL GENERATION AND BAND-STRUCTURE CALCULATION

The calculations are based on the local-density-functional theory.[16] For the exchange and correlation functional, we use the formulation of Hedin and

TABLE I. Nonrelativistic and relativistic valence orbital energies $E_{nl}(j)$ for the Cd and S atoms are calculated self-consistently for the exchange-correlation functionals of HL, $X\alpha$ ($\alpha=1$), and the density-gradient-expansion correction (DGC). SIC eigenvalues are obtained using Eq. (16) in Ref. 30. Values in parentheses are differences in energies between two adjacent average levels. Energies are in eV.

Exchange correlation		HL (Ref. 18)		$X\alpha$ ($\alpha=1$) (Ref. 19)	DGC (Ref. 29)	SIC (Ref. 30)
Relativistic effect		Nonrel.	Rel.	Rel.	Nonrel.	Rel.
Cd E_{5s}	($\frac{1}{2}$)	−5.65	−6.03	−7.29	−6.03	−9.33
		(1.56)	(1.18)	(2.25)	(1.73)	(2.33)
S E_{3p}	($\frac{3}{2}$)	−7.21	−7.17	−9.41	−7.76	−11.63
	($\frac{5}{2}$)		−7.25	−9.51		−11.73
		(5.65)	(4.79)	(7.26)	(5.63)	(7.34)
Cd E_{4d}	($\frac{5}{2}$)	−12.86	−11.71	−16.26	−13.39	−18.67
	($\frac{3}{2}$)		−12.41	−17.03		−19.48
		(4.39)	(5.25)	(3.38)	(4.44)	(3.75)
S E_{3s}	($\frac{1}{2}$)	−17.25	−17.25	−20.18	−17.83	−22.75

Lundqvist (HL).[18] We also test the exchange-"only" potential (Slater exchange with[19] $\alpha=1$) for the atomic and electronic structure calculations, and compare it with the experimental results. This exchange-only potential has been shown (for the CuCl band-structure calculation[20]) to provide better agreement with the observed band gaps than does the more correct local-density-functional treatment with $\alpha=\frac{2}{3}$ for exchange.

To represent the effect of the core states, relativistic norm-conserving pseudopotentials are used. Relativistic effects, i.e., the mass velocity and Darwin terms, in heavy atoms, have been shown to affect significantly the behavior of the valence electrons.[21] Hence it is necessary to consider these effects in generating pseudopotentials for heavier atoms. To generate the relativistic potentials, we use the method proposed by Bachelet and Schlüter,[22] which basically follows the formulation of Kleinman.[23] The l- and s-dependent pseudopotentials are written as[22]

$$V_{\rm ps}^{\rm ion}(\vec{r})=\sum_l |l\rangle[\bar{V}_l^{\rm ion}(\vec{r})+V_l^{\rm so}(\vec{r})\vec{L}\cdot\vec{S}]\langle l| \ , \qquad (1)$$

where

$$\bar{V}_l^{\rm ion}(\vec{r})=\frac{[lv_{l,l-1/2}^{\rm ion}(\vec{r})+(l+1)v_{l,l+1/2}^{\rm ion}(\vec{r})]}{(2l+1)}$$

and

$$V_l^{\rm so}(\vec{r})=\frac{2[v_{l,l+1/2}^{\rm ion}(\vec{r})-v_{l,l-1/2}^{\rm ion}(\vec{r})]}{(2l+1)} \ .$$

For bulk calculations, we use the "j-averaged" potentials $\bar{V}_l^{\rm ion}(\vec{r})$ in Eq. (1), and neglect the spin-orbit term $V_l^{\rm so}(\vec{r})$. The spin-orbit splittings can be expected to affect the S $3p$ and Cd $4d$ states, but not the Cd $5s$ and S $3s$ levels. Experimentally, these splittings for CdS are observed to be 0.065 eV (Ref. 24) for the p-derived and 0.76 eV (Ref. 10) for the d-derived bands. These are close to the atomic splittings (refer to Table I). Since these effects are small, especially for the p state, we ignore the spin-orbit term for the bulk calculation.

To ensure the transferability of the potentials from the atom to the bulk, we require first that the nonrelativistic pseudopotentials[25] reproduce the all-electron energy levels and the wave functions outside the core for several excited configurations for each element. Then, for the heavier Cd atom, the relativistic j-averaged potentials are generated using the same reference configuration as that used in the nonrelativistic case. The pseudoatom calculations are compared with all-electron calculations for excited configurations ranging over 1 Ry for Cd and 2 Ry for S atoms. These pseudopotentials, nonrelativistically generated from the atomic states $5s^{1}5p^{0.5}5d^{0.2}$ for Cd and $3s^{2}3p^{2.5}3d^{0.5}$ for S atoms, reproduce the atomic ground-state and the excited-state energies within 15 mRy for the Cd and 10 mRy for the S atoms.

To investigate the effect of the d states, we include the Cd $4d$ electrons as a valence state. The Cd $4d$ pseudopotential generated from the configuration of $4d^{10}5s^{1}5p^{0.2}$ shows highly localized behavior. In order to make bulk calculations with plane waves easier to converge, we smooth out the peak of the wave function by relaxing the transferability requirement for the pseudopotential as described in Ref. 26. Despite the smoothness of the Cd d potential, it reproduces the atomic ground-state eigenvalues and the excited energies over a 1-Ry range to within 15 mRy.

In the bulk calculation for CdS the Schrödinger equation is solved self-consistently (except for the d-band calculation for the wurtzite) in momentum space.[27] The wave functions without the d electrons in reciprocal space are expanded in terms of plane waves with kinetic energies of up to 13.5 Ry (290 plane waves) for the zinc-blende and

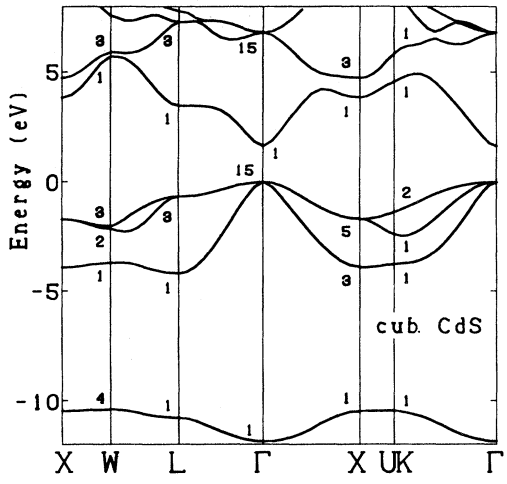

FIG. 1. Electronic band structure for zinc-blende CdS based on the HL functional (not including the d band). Energies are measured from the valence-band maximum $\Gamma_{1,5}$ in units of eV. Numbers refer to the conventional indices for symmetry-group representations.

12 Ry (480 plane waves) for the wurtzite structure, respectively. Convergence test for the zinc-blende calculations has been made by increasing the kinetic-energy cutoff up to 19 Ry (470 plane waves), and the energy eigenvalues changed by less than 0.1 eV. In the d-band calculations, convergence is obtained with a kinetic energy cutoff of 19 Ry for the zinc-blende CdS; the changes in the energy eigenvalues are within 0.1 eV when 230 more plane waves are included (see Table VI). Then the bulk charge-density obtained self-consistently is similar to that of free atoms. For wurtzite CdS including the d band, energies at high-symmetry points are calculated non-self-consistently using 940 plane waves with kinetic energies up to 19 Ry using the residual-minimization method (RMM).[28] Two special $\vec{k}$ points are used for the Brillouin-zone integration. We also tested the energies for 6 $\vec{k}$ points, but the results only changed by less than 0.03 eV. The band-structure calculations were performed using experimental values[4] for the lattice constants of $a=7.8$ a.u. and $c=12.66$ a.u. in the wurtzite structure, and using a lattice parameter of $a=10.96$ a.u. in the zinc-blende structure.[5]

III. RESULTS AND DISCUSSIONS

A. Atomic structures of Cd and S

Table I summarizes the results for the atomic energy levels of Cd and S atoms. Our relativistic and nonrelativistic calculations are performed using several different formulations for the exchange and correlation functional: the local-density functional of HL,[18] the exchange only with $\alpha=1$ (Slater exchange), the density-gradient-corrected[29] (DGC) exchange and correlation, and the simple formula[30] for the self-interaction-corrected (SIC) eigenvalues.[17] The atomic energy levels show that the Cd $4d$ states lie only about 6 eV below the S $3p$ states. Thus we may expect the proximity of these two states to lead to non-negligible d-p interaction. Often, however, the d states are left out of pseudopotential calculations. Relativistic effects do not affect the S valence states, but decrease the Cd $5s$ level by 0.4 eV whereas they increase the Cd $4d$ energy level by 0.9 eV, compared to the nonrelativistic case. Net relativistic effects thus may be expected to yield a reduction of the band gap (difference between the edges of the Cd $5s$—derived and S $3p$—derived bands) by 0.4 eV. Moreover, the motion of the d state closer to the S $3p$ will increase the d-p mixing. For Slater exchange and the SIC, the energy differences between the Cd $4d$ and the S $3p$ are found to increase by about 2.5 eV. This will later be compared to the experimental value for the position of the d bands.

These calculations for the various exchange and correlation functionals are motivated by failures in the LDA in predicting excited and localized states. In particular, this theory underestimates the band gap by 40—50% for solids. In recent years, there have been several attempts to improve the LDA. In Table I we show how two of these, the DGC (Ref. 29) and the SIC,[17,30] affect the results. In the calculation for the SIC orbital energies, we use the simple formulation suggested by Perdew and Norman.[30] We find that the local-density energy levels are substantially changed; the difference in energies between the Cd $5s$ and the S $3p$ increases by 1.1 eV and the Cd $4d$ state is lowered in energy by about 2.5 eV relative to the S $3p$. It is interesting to note that the exchange-only energy differences are quite close to those from the SIC calculation. Since the SIC energy eigenvalues have been reported to be close to the electron removal energies in atoms,[17] we see that the LDA (HL) poorly estimates the localized Cd $4d$ state. Hence, one would expect more d-p interaction to be involved in the valence-band calculation based on the LDA. The inclusion of the DGC in the local exchange-correlation functional (we used the formulation of von Barth and Hedin[31]) increases the difference in energies between the Cd $5s$ and the Cd $4d$ by 0.13 eV and affect slightly the position of the $4d$ state, compared to the nonrelativistic calculation with the HL functional. So one may not expect substantial changes in the band gap and the valence-band width. This arises from the fact that the eigenvalues for Cd and S shift by approximately the same amount. This behavior has also been found in a previous calculation for other atoms.[29]

B. Band structures of CdS

The semirelativistically calculated band structure of zinc-blende CdS is presented in Fig. 1 and that of the wurtzite in Fig. 2. Both exhibit band structures which are similar in shape, bandwidth, and band gap. As expected, the dispersion along Γ—L in zinc blende is very close to that along Γ—A—Γ in wurtzite.[32] The small discrepancies may be caused by the nonideal wurtzite crystal structure that is used. The topology of the zinc-blende band structure is similar to the previous one obtained by the LCAO method.[15] For the wurtzite CdS, the calculated valence-band structure without the d band is presented and compared with the results determined using[1] ARPES in Fig. 3

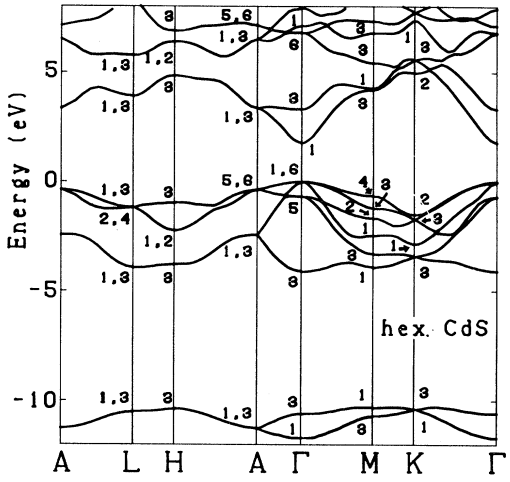

FIG. 2. Band structure for wurtzite CdS based on the HL functional (not including the d band). Energies are measured from the valence-band maximum Γ_1, Γ_6 in units of eV. Numbers refer to the conventional indices for symmetry-group representations.

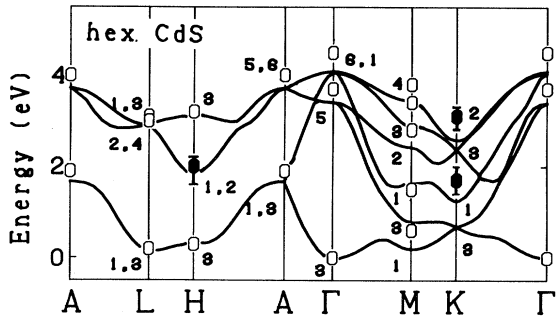

FIG. 3. Upper valence band (solid lines) of wurtzite CdS in Fig. 2 is compared with the ARPES measurements; open circles have uncertainties of ±0.2 eV and closed circles have larger uncertainties as indicated.

and Table II. The general features are similar to the ARPES results. If the zero of energy is taken as the bottom of the valence band, i.e., Γ_3, in Fig. 3, the overall energies are in good agreement with the ARPES results within experimental error except for points at and near Γ_6, i.e., the band edge. Energy differences at and near the band edge probably result from freezing the d state in the valence-band calculation. Further, the topology of our wurtzite valence-band structure is similar to that of the EPM calculation[3] rather than that of the OPW results.[2] For the wurtzite conduction band we compare the present results with those using the OPW method in Table III. Our calculations resemble the OPW results if all the unoccupied states are shifted up by about 1 eV.

In Table IV, the numerical results for the CdS band structures are presented and compared with other theoretical and experimental values. Although the calculated direct gaps (Γ_1, Γ_6 to Γ_1 in the wurtzite and $\Gamma_{1,5}$ to Γ_1 in the zinc blende) are found to be at the proper points in $\vec{k}$ space, their energy values are underestimated by about 30% (including relativistic effects but without the d band) compared to the experimental value of 2.55 eV.[6,7] This is consistent with results for other band-structure calculations[33] using the LDA. As expected from the atomic structure calculations, relativistic corrections reduce the band gap by 0.3—0.4 eV and increase the p-derived valence-band width by 0.2 eV. However, the p-derived valence-band widths keeping the d band frozen (4.2 eV for the zinc blende and 4.1 eV for the wurtzite) are underestimated by 0.3—0.4 eV compared with the ARPES measurement and by 0.8 eV compared with the XPS (Ref. 8) result. In comparison with other wurtzite calculations, using the OPW (3.3 eV) method and the EPM (3.0 eV), our valence-band width of 4.1 eV is substantially improved. Moreover, we find that this valence-band width is drastically improved when the d band is included as a valence state. We will discuss the effects of the d states on the valence band in the next section.

TABLE II. Comparison of the p-derived valence-band energies with the ARPES results (Ref. 1) for hexagonal CdS. Self-consistent (SC) calculation includes relativistic effects but not the d band. Non-self-consistent (NSC) energies are obtained by including the d band but not relativistic effects. Energies are in eV from the Γ_3 point. Experimental errors are ±0.2 eV.

$\vec{k}$ point	SC	NSC	ARPES	$\vec{k}$ point	SC	NSC	ARPES
Γ_6	4.1	5.1	4.5	M_3	0.8	1.1	1.5
Γ_1	4.0	5.0		M_1	0.2	0.5	0.6
Γ_5	3.4	4.0	3.7	$A_{5,6}$	3.7	4.5	4.0
Γ_3	0	0	0	$A_{1,3}$	1.7	2.3	1.9
$L_{1,3}$	2.9	3.3	3.1	H_3	3.1	3.5	3.2
$L_{2,4}$	2.9	3.3	3.0	$H_{1,2}$	1.8	2.0	2.0(+0.2, −0.4)
$L_{1,3}$	0.1	0.5	0.2	H_3	0.3	0.6	0.3
M_4	3.5	4.0	3.8	K_2	2.6	3.0	3.1(+0.2, −0.3)
M_3	2.9	3.4	3.4	K_3	2.4	2.7	
M_2	2.4	2.6	2.8	K_1	1.3	1.2	1.7±0.3
M_1	1.6	1.8		K_3	0.7	1.0	

TABLE III. Comparison of the eigenvalues for the unoccupied band energies with the OPW (Ref. 2) results for hexagonal CdS. Calculation includes relativistic effects but not the d band. Energies are in eV.

$\vec{k}$ point	OPW	LDA (HL)	$\vec{k}$ point	OPW	LDA (HL)
Γ_1	2.50	1.77	H_3	5.82	4.84
Γ_3	4.27	3.29	$H_{1,2}$	7.25	6.39
Γ_6	7.70	6.80	M_3	5.12	4.19
Γ_1	8.01	7.11	M_1	5.44	4.27
$A_{1,3}$	4.19	3.34	M_3	6.36	5.42
$A_{1,3}$	7.35	6.51	$L_{1,3}$	4.78	3.89
K_2	6.05	5.00	$L_{1,3}$	6.91	5.76
K_3	6.80	5.58			

TABLE IV. Comparison of the electronic structures with experimental and other theoretical results for cubic and hexagonal CdS. E_g, $\Delta E(p)$, and $\Delta E(s)$ denote the band gap, the p- and s-derived bandwidths. ΔE_v, ΔE_d, and $\langle E_\Gamma - E_d \rangle$ denote the valence-band width, the d-band width, and the average position of the d band at the Γ point relative to the main valence-band edge. Energies are in eV.

	E_g	$\Delta E(p)$	$\Delta E(s)$	ΔE_v	$\Delta E(d)$	$\langle E_\Gamma - E_d \rangle$
			Cubic CdS			
Present results						
HL (Nonrel. without d)	1.93	4.0	1.3	11.76		
HL (Nonrel. with d)	0.67	5.06	0.70	12.84	1.18	8.38
HL (Rel. without d)	1.65	4.17	1.4	11.80		
HL (Rel. with d)	0.30	5.30	0.84	13.00	1.19	7.78
$X\alpha$ (Rel. without d)	2.25	3.45	1.0	11.77		
$X\alpha$ (Rel. with d)	1.01	4.41	0.44	12.68	1.06	9.72
Other calculations						
LCAO (Ref. 15)	2.01	5.11	0.57	12.27	0.9	9.9
OPW (Ref. 12)	2.6	2.2	0.1	12.30		10.0
			Hexagonal CdS			
Present results						
HL (Rel. without d)	1.77	4.1	1.32	11.69		
Other calculations						
OPW (Ref. 5)	2.5	3.3	0.99	11.49		16.5
EPM (Ref. 6)	2.6	3.0				
Experiments	2.55[a]	4.5±0.2[b]		12.5[d]		9.64[c]
		5.0±0.4[c]				10.10[e]
						10.00[e]
						10.70[f]
						9.20[g]

[a]UPS (Refs. 6 and 7).
[b]ARPES (Ref. 1).
[c]XPS (Ref. 8).
[d]XPS (Ref. 37).
[e]XPS and UPS (Ref. 9).
[f]UPS (Ref. 10).
[g]UPS (Ref. 11).

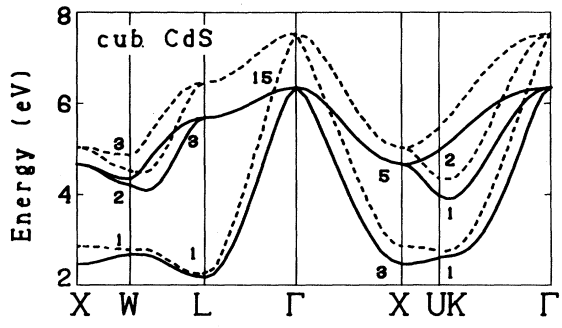

FIG. 4. Effects of the d band (dashed lines) on the upper valence band for zinc-blende CdS based on the HL functional (including relativistic effects). Energy scales are arbitrary.

C. d-p and d-s interactions

We have investigated the role of the d band in the formation of the CdS band structures by treating the d state as a valence state. In previous calculations for hexagonal CdS both the OPW and EPM methods have been reported to underestimate the p-derived bandwidth despite the successful predictions of the fundamental gaps and the optical spectra. This underestimate has also been found in other calculations[12] for cubic zinc- and cadmium-based compounds compared to the experimental data.[8] Since the d band in these material has localized behavior and thus a narrow width, one may neglect the d interaction with the valence state to make the plane-wave convergence easier. Recently the modified tight-binding approximation[34] for cubic AgI has shown that the d-p interaction tends to improve the p-derived bandwidth. Experimentally the low-binding-energy peak in the photoemission spectrum of the d level of CdS(1120) (Ref. 35) indicates more possible mixing of the d band with the valence electrons. This weak peak has not been observed on the metallic d core level. It appears that the d state must be incorporated into the valence-band calculation if a reliable band structure is to be expected.

In Fig. 4 the effects of the d band on valence-band formation are shown. We find that inclusion of the d-p interaction drastically affects the energies near the band edge Γ_{15} and at L_3 whereas it changes slightly the lower energies located at the points W_1, L_1, X_3, and K_1. The maximum effect of the d band occurs at the Γ_{15} point. The d-p hybridization shifts the Γ_{15} point to higher energy, but it only causes a slight change in the conduction-band edge. Thus, the d band induces an improved valence-band width and a smaller band gap. The same behavior has also been found in the AgI band-structure calculation by Smith.[34] The values quoted here are all obtained using the local-density exchange-correlation functional (HL), however, the effect of the d bands is similar for the exchange-only functional. The self-consistent value of 5.3 eV for the valence-band width of cubic CdS is in good accord with the hexagonal XPS data[8] within experimental error, but is larger than that derived from ARPES.[1] This calculated value is close to the LCAO (Ref. 15) result of 5.1 eV. The position of the d band is found to be 7.8 eV below the valence-band edge. This is about 2 eV above the experimental value for hexagonal CdS, i.e., 9.2–10.7 eV.[8–11] A similar error has also been found in a previous cubic ZnS band-structure calculation[36] based on the LDA. The d-band width of 1.2 eV obtained here is close to the LCAO result of 0.9 eV. Non-negligible d-s hybridization has also been found to reduce the s-derived bandwidth from 1.4 to 0.8 eV, which is close to the LCAO result of 0.6 eV. Our calculated value for the valence-band width, i.e., 13 eV, is in better agreement with the experimental value of 12.5 eV (Ref. 37) when compared to 11.8 eV obtained by excluding the d band.

For wurtzite CdS, the self-consistent calculations are computationally impractical at this point because they re-

TABLE V. Non-self-consistent electronic structure including the d band for wurtzite CdS. For the zinc-blende structure, non-self-consistent results are compared with the self-consistent case. The exchange-correlation functional of HL is used. Energies are in eV.

	E_g	$\Delta E(p)$	$\Delta E(s)$	ΔE_v	$\Delta E(d)$	$\langle E_\Gamma - E_d \rangle$
Cubic Cds						
Self-consistent nonrelativistic	0.67	5.06	0.70	12.84	1.18	8.38
Self-consistent relativistic	0.30	5.30	0.84	13.00	1.19	7.78
Non-self-consistent nonrelativistic	0.60	5.18	0.81	12.99		7.21
Non-self-consistent relativistic	0.25	5.49	0.93	13.41		
Hexagonal CdS						
Non-self-consistent nonrelativistic	0.77	5.07	0.80	12.88		6.86
Non-self-consistent relativistic	0.30	5.37	0.91	13.07		6.50

TABLE VI. Comparison of the non-self-consistent (NSC) p-derived valence-band energies with the self-consistent (SC) ones for cubic CdS. Self-consistent energies are obtained with kinetic-energy cutoffs of 19 and 25 Ry. Energies are in eV from the L_1 point.

$\vec{k}$ point	NSC (19 Ry)	SC (19 Ry)	SC (25 Ry)	$\vec{k}$ point	NSC (19 Ry)	SC (19 Ry)	SC (25 Ry)
Γ_{15}	5.49	5.33	5.27	W_2	2.26	2.30	2.29
X_3	0.90	0.52	0.61	W_3	2.74	2.62	2.61
X_5	2.83	2.84	2.79	K_1	0.65	0.53	0.53
L_1	0	0	0	K_1	2.18	2.12	2.12
L_3	4.34	4.25	4.21	K_2	3.30	3.23	3.22
W_1	0.69	0.55	0.55				

quire twice the number of plane waves as that used for zinc blende. However, we have obtained the non-self-consistent energies by diagonalizing the secular matrix using the RMM.[28] In the comparison with the results for cubic CdS (see Tables V and VI), non-self-consistent eigenvalues are close to the self-consistent ones. By considering the equivalence[32] of two axes, Γ-L (zinc blende) and Γ-A (wurtzite), we can expect an equivalent effect for the d band along the Γ-A axis as that obtained for the Γ-L axis. The energy at Γ_3 (wurtzite), which corresponds to L_1 (zinc blende), will be unaffected whereas the Γ_1 will be shifted to higher energy by approximately the same amount as that obtained at Γ_{15} (zinc blende). As discussed before, the inclusion of the d band in the wurtzite structure improves the main-valence-band width by about 1.2 eV. The improved value is almost equal to the XPS result. Non-self-consistent valence-band energies (without relativistic effects) are given in Table II and compared with the ARPES results. We find that the discrepancies in the energies are reduced by incorporating the d band into the valence states. Small errors of 0.3—0.4 eV in the lower energies at $L_{1,3}$, $A_{1,3}$, and H_3 result from the non-self-consistent effect because for cubic CdS the lower energies non-self-consistently obtained at X_3, W_1, and K_1 are slightly higher than the self-consistent ones (see Table VI).

The fact that the d band is not narrow indicates non-negligible d-p interaction, and is in good agreement with the experimental evidence[35] of a broad d band. The underestimation of the position of the d band in the LDA may be interpreted to indicate that more d-p interaction and thus a larger valence-band width is needed. This is the reason why the main-valence-band width calculated using the LDA is larger by 0.8 eV compared to the ARPES measurement and by 0.3 eV to the XPS result. This fact can be verified by examining the exchange-only calculation. In fact, this functional yields the atomic energy levels closer to the SIC calculations. In the band-structure calculation with $\alpha=1$, the main-valence-band width of 4.4 eV, the position of the d band of 10.0 eV, and the valence-band width of 12.7 eV are in better agreement with the hexagonal experimental data, compared to those obtained from the local-density functional. Clearly, accurate positioning of the d band remedies some errors in the valence-band features based on the local-density exchange-correlation functional. However, the band gap is still significantly underestimated because the calculation is based on the LDA. In recent years, corrected local-density-functional theories have been reported to improve the band gaps and localized states. In the nonlocal-density approximation to exchange correlation the conduction bands are shifted to higher energies with respect to the Fermi level, and thus is in reasonable agreement with experimental data for Rh (Ref. 38) and Si.[39] The application of the SIC LDA to LiCl (Ref. 40) substantially improved the band gap and core levels. The use of these corrections may be expected to improve our band gap and the position of the d band.

IV. SUMMARY

We have obtained reasonably accurate band structures for wurtzite and zinc-blende CdS based on the LDA even without including the effects of the d band. Inclusion of the d state as a valence state has been found to improve some valence-band features in the wurtzite and zinc-blende structures. We find that the maximum effect of the d-p interaction occurs at the valence-band edge, and the non-negligible d-s interaction reduces the s-derived bandwidth in both structures of CdS. However, the inaccuracies in describing the localized d states using the LDA produces systematic error in the valence-band properties.

ACKNOWLEDGMENTS

We are grateful to N. G. Stoffel and G. Margaritondo for providing us with the angle-resolved Cd 4d spectra. This work was supported by the National Science Foundation under Grant No. DMR-78-22465 and by the Director, Office of Energy Research, Office of Basic Energy Sciences, Materials Sciences Division of the U.S. Department of Energy, under Contract No. DE-AC03-76SF00098.

[1]N. G. Stoffel and G. Margaritondo (unpublished).
[2]R. N. Euwema, T. C. Collins, D. G. Shankland, and J. S. Dewitt, Phys. Rev. 162, 710 (1967).
[3]T. K. Bergstresser and M. L. Cohen, Phys. Rev. 164, 1069 (1967).
[4]D. G. Thomas and J. J. Hopfield, Phys. Rev. 116, 573 (1959).
[5]R. W. G. Wyckoff, *Crystal Structure* (Wiley, New York, 1963), and references therein.
[6]M. Cardona and G. Harbeke, Phys. Rev. 137, A1467 (1965).
[7]M. Cardona, M. Weinstein, and G. A. Wolff, Phys. Rev. 140, A633 (1965).
[8]L. Ley, R. A. Pollak, F. R. McFeely, S. P. Kowalczyk, and D. A. Shirley, Phys. Rev. B 9, 600 (1974).
[9]C. J. Vaseley, R. L. Hengehold, and D. W. Langer, Phys. Rev. B 5, 2296 (1972).
[10]C. J. Vaseley and D. W. Langer, Phys. Rev. B 4, 451 (1971).
[11]J. L. Shay and W. E. Spicer, Phys. Rev. 169, 650 (1968).
[12]S. I. Kurganskii, O. V. Faverovich, and E. P. Domashevskaya, Fiz. Tekh. Poluprovodn. 14, 1315 (1980) [Sov. Phys.—Semicond. 14, 775 (1980)].
[13]D. J. Stukel, R. N. Euwema, T. C. Collins, F. Herman, and R. L. Kortum, Phys. Rev. 179, 740 (1969).
[14]F. Herman, R. L. Kortum, C. D. Kuglin, J. P. Van Dyke, and S. Skillman, Methods Comput. Phys. 8, 193 (1968).
[15]A. Zunger and A. J. Freeman, Phys. Rev. B 17, 4850 (1978).
[16]P. Hohenberg and W. Kohn, Phys. Rev. 136, B864 (1964); W. Kohn and L. J. Sham, *ibid.* 140, A1133 (1965).
[17]J. P. Perdew and A. Zunger, Phys. Rev. B 23, 5048 (1981).
[18]L. Hedin and B. I. Lundqvist, J. Phys. C 4, 2064 (1971).
[19]J. C. Slater, Phys. Rev. 81, 385 (1951).
[20]L. Kleinman and K. Mednick, Phys. Rev. B 20, 2487 (1979).
[21]N. C. Phyper, Mol. Phys. 39, 1327 (1980).
[22]G. B. Bachelet and M. Schlüter, Phys. Rev. B 25, 2103 (1982).
[23]L. Kleinman, Phys. Rev. B 21, 2630 (1980).
[24]U. Rössler, Phys. Rev. 184, 733 (1969), and references therein.
[25]D. R. Hamann, M. Schlüter, and C. Chiang, Phys. Rev. Lett. 43, 1494 (1979).
[26]K. J. Chang, S. Froyen, and M. L. Cohen, J. Phys. C 16, 3475 (1983).
[27]J. Ihm, A. Zunger, and M. L. Cohen, J. Phys. C 12, 4409 (1979).
[28]P. Bendt and A. Zunger (unpublished).
[29]D. C. Langreth and M. J. Mehl, Phys. Rev. Lett. 47, 446 (1981); Phys. Rev. B 28, 1809 (1983).
[30]J. P. Perdew and M. R. Norman, Phys. Rev. B 26, 5445 (1982).
[31]U. von Barth and L. Hedin, J. Phys. C 5, 1629 (1972).
[32]J. L. Birman, Phys. Rev. 115, 1493 (1959).
[33]M. T. Yin and M. L. Cohen, Phys. Rev. B 26, 5668 (1982).
[34]P. V. Smith, Phys. Status Solidi 37, 589 (1976).
[35]N. G. Stoffel and G. Margaritondo (private communication).
[36]P. Bendt and A. Zunger, Phys. Rev. B 26, 3114 (1982).
[37]E. P. Domashevskaya, V. A. Terekhov, L. N. Marshakova, Ya. A. Ugai, V. I. Nefedov, and N. P. Sergushin, J. Electron Spectrosc. Relat. Phenom. 9, 261 (1976).
[38]G. Borstel and M. Newmann, Phys. Rev. B 23, 3113 (1981).
[39]G. P. Kerker, Phys. Rev. B 24, 3468 (1981).
[40]R. A. Heaton, J. G. Harrison, and C. C. Lin, Solid State Commun. 41, 827 (1982).